Iğdır Üniversitesi Fen Bilimleri Enstitüsü Dergisi, 14(2), 822-834, 2024
Journal of the Institute of Science and Technology, 14(2), 822-834, 2024

ISSN: 2146-0574, eISSN: 2536-4618

Kimya / *Chemistry* **DOI: 10.21597/jist.1416223**

Araştırma Makalesi / *Research Article*

Geliş tarihi / *Received*: 08.01.2024 **Kabul tarihi / *Accepted*: 12.02.2024**

Atıf İçin: Gören, K., Bağlan, M., Yıldıko, Ü. ve Tahiroğlu, V. (2024). Anti-Kanser ve Anti-Üreaz Aktivitesi için Tiazolidinon-Bis Schiff Bazının Moleküler Yerleştirme ve DFT Analizi. *Iğdır Üniversitesi Fen Bilimleri Enstitüsü Dergisi*, 14(2), 822-834.

To Cite: Gören, K., Bağlan, M., Yıldıko, Ü. & Tahiroğlu, V. (2024). Molecular Docking and DFT Analysis of Thiazolidinone-Bis Schiff Base for anti-Cancer and anti-Urease Activity, *Journal of the Institute of Science and Technology*, 14(2), 822-834.

Anti-Kanser ve Anti-Üreaz Aktivitesi için Tiazolidinon-Bis Schiff Bazının Moleküler Yerleştirme ve DFT Analizi

Kenan GÖREN[1], Mehmet BAĞLAN[1], Ümit YILDIKO[2], Veysel TAHİROĞLU[3*]

Öne Çıkanlar:
- DFT optimizasyonu
- Kanser karşıtı
- Schiff Baz

Anahtar Kelimeler:
- DFT
- NBO
- MEP
- Moleküler Yerleştirme
- Tiazolidinon-Bis Schiff Bazı

ÖZET:

Bu araştırma (2Z,5E)-2-(((E)-benziliden)hidraziniliden)-5-(nitro(fenil)metilen)-3-feniltiazolidin-4-on molekülün (Tiazolidinon-Bis Schiff Bazı) yapısal karakterizasyonuna odaklanmıştır. Molekülün kararlı faz geometrisine dayanarak yapısal karakterizasyon için SDD ve 6-311++G(d,p) temel setleri ile B3PW91 tekniği kullanılarak tüm hesaplamalar yapıldı. Çalışmamızda yörüngeler arası ve yörüngeler arası bağ etkileşimleri, HOMO-LUMO enerji boşlukları ve Tiazolidinon-Bis Schiff Bazı'ın elektrostatik yüzey haritalama işlemleri dahil olmak üzere birçok hesaplama gerçekleştirildi. Daha sonraki bir araştırmada, protein üzerindeki ligandın özel bağlanma bölgesini ve mekanizmasını analiz etmek için moleküler yerleştirmeyi kullandık. Schiff Thiazolidinone Kansere ve üreaz enzimlerine karşı moleküler yerleştirme sonuçları elde edildi.

Molecular Docking and DFT Analysis of Thiazolidinone-Bis Schiff Base for anti-Cancer and anti-Urease Activity

Highlights:
- DFT Optimization
- Anti-Cancer
- Schiff Base

Keywords:
- DFT
- NBO
- MEP
- Molecular Doking
- Thiazolidinone-Bis Schiff Base

ABSTRACT:

This reearch focused on the structural characterization of (2Z,5E)-2-(((E)-benziliden) hidraziniliden)-5-(nitro(fenil)metilen)-3-feniltiazolidin-4-on molecule (Thiazolidinone-Bis Schiff Base). Depending on the molecule's stability phase geometry, all analyses have been carried out utilizing the B3PW91 technique with 6-311++G(d,p) and SDD basis sets, for structural characterisation. Many computations were performed in our work, including inter-orbital and inter-orbital bond interactions, HOMO-LUMO energy deficiencies, and electrostatic surface mapping processes of the Thiazolidinone-Bis Schiff Base. In a subsequent investigation, we have used molecular docking to analyze the particular binding place and method of the ligand onto the protein. Schiff Thiazolidinone Molecular docking results against cancer and urease enzymes were obtained.

[1]Kenan GÖREN (**Orcid ID:** 0000-0001-5068-1762), Mehmet BAĞLAN (**Orcid ID:** 0000-0002-7089-7111), Kafkas University, Department of Chemistry, Kars, Türkiye.
[2]Ümit YILDIKO (**Orcid ID:** 0000-0001-8627-9038), Kafkas University, Department of Bioengineering, Kars, Türkiye.
[3]Veysel TAHİROĞLU * (**Orcid ID:** 0000-0003-3516-5561), Şırnak University, Faculty of Health Sciences, Department of Nursing, Şırnak, Türkiye.

****Sorumlu Yazar/*Corresponding Author*:** Veysel TAHİROĞLU, e-mail: veysel.tahiroglu@sirnak.edu.tr

INTRODUCTION

Chemistry has historically been an experimental discipline. Previously, before working with any molecule, it was investigated in its natural state or manufactured (Goh et al., 2017). These research have been carried out owing to advancements in computer hardware and software, and investigations in the field of computational chemistry have been carried out more readily without such constraints (Kaltsoyannis, 2018). In this manner, the computational investigation of a molecule whose characteristics are sought to be evaluated is possible. Theoretical chemistry is a discipline of chemistry that uses mathematical approaches to describe chemistry (Pyykkö, 2005). Computational chemistry is a discipline of chemistry that uses computer hardware and software to solve chemical issues (Rupp et al., 2018). In general, theoretical chemists tackle chemical issues largely with software or programs that employ mathematical methods, and they interpret the results obtained with these software or programs, so forming a link between experimental and theoretical chemistry (Pang & Reed, 1998). To compute the structure and characteristics of molecules, they frequently employ theoretical chemistry methods. In computational chemistry, in addition to stable molecules, unstable, short-lived products, and even intermediate intermediates can be explored, as well as their transition states (Topsom, 1983). The results of computational chemistry are often understood as the outcome of experimental investigations, and sometimes undiscovered chemical events can be anticipated (Cuesta et al., 2006).

Hugo Schiff described process of condensation between an aldehyde and an amine to produce a Schiff base. Because of the presence of the imine group, Schiff bases are employed to understand the transformation process of the racemization reaction in biological systems (da Silva et al., 2011). It exhibits anticancer, antibacterial, antifungal, herbicidal, and other effects as a result of the existence of the azomethine linkage (>C=N-) in living systems. Various biological activities, such as, are being studied. Because of their potent antibacterial, antifungal, and antiviral activities, several Schiff derivatives are effective medicinal medicines (Berhanu et al., 2019). Furthermore, Schiff bases and their analogs are commonly utilized as model compounds to study the structure-activity connection of biomolecules and pharmacological molecules (Hodnett & Dunn, 1970).

Bis-Schiff base and Thiazolidinone are two " well-off" nitrogen-containing compounds with extensive use in medicines and pharmaceuticals. Anti-convulsant, anti-bacterial, anti-tuberculosis, anti-glycation, anti-epileptic scaffolds are some examples. It is capable of a diverse range of biological activities including (Preeti et al., 2023). A hybrid compound incorporating thiazolidinone bis-Schiff base systems is viewed as potential relevant, and its production under ecologically friendly circumstances is worth researching (Al-Sharif, 2023).

Quantum chemical computations are useful approaches for building NLO molecules and for predicting some features of novel supplies, like polarizability, molecular dipole moments, and hyperpolarizability (Assfeld & Rivail, 1996). We report the atomic structure, natural bond orbital (NBO) analysis and NLO, molecular electrostatic potential (MEP) maps, and molecular surfaces of the title molecule in the initial condition, as well as DFT using 6-311G++(d,p) and SDD basis sets, in this paper. The /B3PW91 procedure was used to do the necessary computations. The open DFT/B3PW91/ SDD/6-311G++(d,p) technique was utilized to determine whole energy, HOMO and LUMO energies, $\Delta E_{LUMO-HOMO}$ energies, and $\Delta E_{LUMO-HOMO}$ energies.

Urease is a nickel-rely metalloenzyme which catalyzes the urea deteriorate, producing carbon dioxide and ammonia. Changing the pH of an aqueous solution to allow Helicobacter pylori to produce ammonia boosted the bacteria's survivability (Mobley, 2001). In addition, Helicobacter pylori has been found to be the fundamental root of a variety gastroduodenal dysfunctions. These illnesses include

duodenal ulcers, stomach cancer, peptic ulcers, and urinary catheter encrustation (Tabatabai & Bremner, 1972). Urease inhibitors can shield you in the case of ureolytic infections caused by bacteria. Maintain control over urea degradation. Because of the biological importance of organic heterocyclic compounds that serve as, medicinal chemists, urease enzyme inhibitors have spent a substantial time and effort developing novel heterocyclic urease inhibitors as prospective therapeutic alternatives (Qin & Cabral, 2002). For numerous decades, urea and hydroxamic acid compounds, coumarin, triazole, semicarbazone, Schiff bases, piperidine, and oxadiazole have been used to cure gastroduodenal illness by blocking the urea enzyme (Polacco & Holland, 1993). Antifreeze compounds have also been discovered and have piqued the interest of medical experts due to their ability to inhibit urease enzymes. The investigation of biological activity and pharmaceutical production are both heavily reliant on N-Containing Heterocyclic molecules (Callahan et al., 2005).

In our study, many DFT calculations of Thiazolidinone-Bis Schiff Base were performed using two methods and basis sets, including inter-orbital and inter-orbital bond interactions, HOMO-LUMO energy gaps, structural characterization of the molecule based on stable phase geometry, and Mulliken Atomic Charges. In this study, molecular modeling studies were also carried out and molecular docking results against cancer and urease enzymes were obtained.

MATERYAL VE METOT

The full DFT calculation was performed in Gaussian 09 program utilizing theory levels B3PW91/6-311++G(d,p)-SDD. The form of the generated compound has been modified as a first step in computer work. For Thiazolidinone-Bis Schiff Base, minimal energy sensitive to molecular shape shifts caused by nuclear location dislocation is required. The DFT approach of Gaussian 09 has been used for calculating the molecular structure of Thiazolidinone-Bis Schiff Base and the energies of the best geometries (Michael J. Frisch, 2016). The basis set is the Lee's-Yang-Parr association functional, which depends on the SDD software program. Molecular docking (Maestro Molecular Modeling system (versioning 11.8) of Schrödinger, LLC model) was employed to explore the exact interaction site and the ligand's method of action on the protein (Verma et al., 2023). The prior Ligprep module implementation was used to synthesis all compounds. Using the wizard module, protein preparation was halted to gather data. At this time, every molecule of water have been emptied from the structure of the crystal. This module was utilized to change the the protein ion concentration again, this time by by determining the protein's the site that was responsible to elastic binding. Mesh blocks served as the sensor grid compound's foundation, establishing circuits in protein site binding and permitting for variable docking. The slip inserting mechanism was utilised to create a ligand-protein docking approach. Using ligand-protein relationships, hydrogen bonds, and alkyl and alkyl connections, optimal binding energies were estimated. The lowest energy designs have the highest affinity for binding. Using Discovery Studio 4.5, the generated receptor model, as well as 2D and 3D interactions, were displayed (El-Hassab et al., 2020).

RESULTS AND DISCUSSION

Structure Details and Analysis

Table 1 shows the ideal structural variables determined utilising the DFT/B3PW91 approach and the 6-311++G(d,p) and SDD basis packages. B3PW91 has been utilized to compare bond lengths and angles optimized by the procedure to those optimized by the two basis sets. When the bond lengths between the molecule's C-O elements are determined using the two methodologies, B3PW91-6-311G++(d,p) is calculated as 1.204 in theory and basis set, and 1.240 in B3PW91-SDD theory and basis

set. The bond length was shorter in the first procedure. Both techniques can employ bond lengths in aromatic and aliphatic structures. Because of the delicate of the procedures, there has been minor variances between the procedures. Both strategies are comparable as shown in Table 1. The calculated C18–H41 (1.08427 Å) bond lengths is quite short contrasted to other bond distances. Bond lengths of C8-O18 (1.204), C8N7 (1.401), and C11S10 (1.772) in the thiazolidine ring were estimated using DFT. As seen in Table 1, both computed approaches agree with the bond angles. When the bond angles in the two approaches were compared, the largest difference was found in C8-N7-O11 atoms, whereas the biggest difference in dihedral structures was found in C13-C11-N29-O30 atoms.

Table 1. Some bond angles (°) and bond lengths (Å) of our theoretically examined molecule

Bond Lengths	B3PW91/ 6-311++G (d,p)	B3PW91/ SDD	Bond Lengths	B3PW91/ 6-311++G(d,p)	B3PW91/ SDD
C4-N7	1.44088	1.45127	**C21-C22**	1.45685	1.46210
C8-C9	1.48998	1.49058	**C23-C24**	1.38990	1.40225
C8-O28	1.20414	1.24038	**C25-C26**	1.39568	1.40879
C11-S10	1.77283	1.83280	**N29-O31**	1.21036	1.26344
C12-N29	1.49155	1.49710	**C18-H41**	1.08427	1.08603
N29-O30	1.21460	1.26829	**C14-H37**	1.37067	1.08630
C12-C13	1.46717	1.47296	**C16-H39**	1.08489	1.08640
C11-N19	1.27996	1.29135	**C21-H42**	1.09488	1.09538
N19-N20	1.37540	1.41311	**C23-H43**	1.08630	1.08835
N20-C21	1.28432	1.30540	**C26-H46**	1.84342	1.08676
Bond Angles	**B3PW91/ 6-311++G (d,p)**	**B3PW91/ SDD**	**Bond Angles**	**B3PW91/ 6-311++G(d,p)**	**B3PW91/ SDD**
C2-C1-C6	120.02979	120.01953	**C9-C12-C13**	128.22986	128.94810
C3-C4-N7	119.44571	119.37889	**O29-N30-O31**	126.63555	125.61825
C8-N7-C11	116.11596	117.06890	**C11-N19-N20**	117.01025	118.03966
N7-C8-O28	123.92858	123.46060	**N19-N20-C21**	112.13906	111.55621
C9-S10-N11	91.89163	90.77631	**N21-C22-C23**	122.34262	118.91624
Planar Bond Angles	**B3PW91/ 6-311++G(d,p)**	**B3PW91/ SDD**	**Planar Bond Angles**	**B3PW91/ 6-311++G(d,p)**	**B3PW91/ SDD**
C5-C4-N7-C8	88.31237	87.36642	**C13-C12-C9-S10**	-3.29187	-4.25097
C4-N7-C8-O28	1.69077	1.58244	**C11-N19-N20-C21**	-179.38472	179.96750
C12-C9-C8-N28	-4.48896	-5.06280	**N19-N20-C21-C22**	179.93651	179.95914
C13-C11-N29-O30	90.35914	93.30635	**C21-C22-C27-C26**	-179.95949	-179.97307

Mulliken Atomic Charges

Mulliken estimations of atomic charge are frequently used in quantum chemistry computations (Hratchian et al., 2008). Mulliken charge polarization, stability, electronic structure, and so on. It may be used to generate several ideas (Kar & Sannigrahi, 1988). It further demonstrates how molecular charge transfer and charge sharing may aid in the formation of electron donor-acceptor pairs (Parandekar et al., 2008). Mulliken loads for our compound were estimated using the theory and basis sets B3PW91/6-311G++(d,p) and B3PW91/SDD, and have been shown in Table 2. In addition, we obtained photos of a) Structure Optimization, b) Atomic Mass, c) Bond Lengths, and d) Mulliken Loads utilising the DFT/B3PW91/6-311++G(d,p) technical and basis set and provided them in Figure 1. S10 (-0.065)-(0.319) and N7 (0.775)-(-0.426) Mulliken charges are connected to the thiazolidine ring. As we've seen, certain C atoms are positive while others are negative. All of the hydrogen atoms recovered from Mulliken analysis have positive charges ranging from 0.1590.235. Nitrogen atoms N20 (-0.261), N29 (-0.354), and oxygen atoms O28 (-0.030) and O31 (-0.048) all have negative charges and operate just like acceptors of electrons.

Table 2. Mulliken atomic charges of Thiazolidinone-Bis Schiff Base

ATOMS	B3PW91/ 6-311++G(d,p)	B3PW91/ SDD	ATOMS	B3PW91/ 6-311++G(d,p)	B3PW91/ SDD
C1	-0.552	-0.239	**N19**	0.429	-0.011
C2	0.014	-0.220	**N20**	-0.261	-0.080
C3	0.254	-0.324	**N29**	-0.354	0.055
C4	-1.311	0.584	**O28**	-0.030	-0.191
C5	0.071	-0.324	**O30**	0.184	-0.190
C6	-0.185	-0.218	**O31**	-0.048	-0.163
N7	0.775	-0.426	**H32**	0.161	0.227
C9	-0.757	-0.474	**H33**	0.171	0.226
S10	-0.065	0.319	**H34**	0.223	0.234
C11	-0.261	-0.212	**H35**	0.201	0.235
C12	0.388	0.399	**H36**	0.187	0.226
C13	0.639	0.296	**H38**	0.181	0.231
C14	-0.251	-0.350	**H39**	0.169	0.233
C15	-0.447	-0.222	**H40**	0.194	0.230
C16	-0.103	-0.225	**H42**	0.182	0.232
C18	-0.387	-0.346	**H43**	0.159	0.223

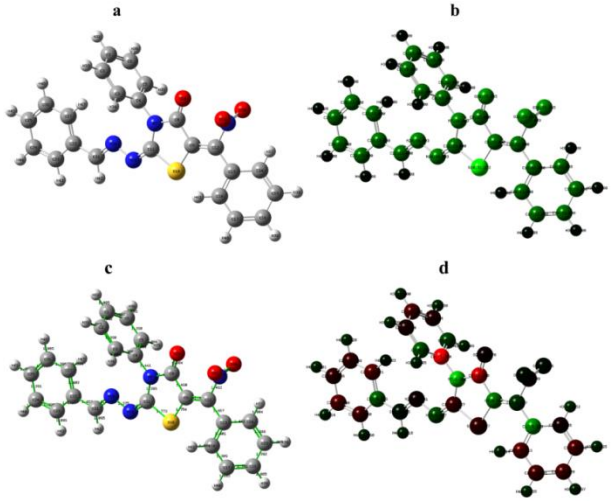

Figure 1. Thiazolidinone-Bis Schiff Base Compound with basis set DFT/B3PW91/6-311++G(d,p) a) Structure Optimization, b) Atomic Mass, c) Bond distance d) Mulliken Charge

HOMO and LUMO Analysis

Frontier orbitals of molecules are classified into two types: highest and occupied chemical orbits (HOMOs) and lowest and empty molecular orbitals (LUMOs) (Suhasini et al., 2015). According to frontier orbital theory, an inhibitor molecule's capacity to donate electrons is often tied to HOMO (Demir & Akman, 2017). High E_{HOMO} values demonstrate a molecule's capacity to give electrons. E_{LUMO} has demonstrated the capacity of molecules to take electrons. HOMO and LUMO frontier orbitals utilising the theory and sets DFT/B3PW91/6-311++G(d,p) and DFT/B3PW91/SDD of Thiazolidinone-Bis Schiff Base compound are determined in Figure 2-3. Table 3 also includes the quantum chemical parameters derived using DFT/B3PW91/6-311++G(d,p)-DFT/B3PW91/SDD techniques for the minimal energy forms of Thiazolidinone-Bis Schiff Base. In the two basis sets utilized in the molecule, the values estimated as E_{HOMO}=-6.2669 eV/-6.3771 eV and E_{LUMO}=-2.7752eV/-2.9915eV were found to be in close agreement. In the two sets employed, E_{HOMO-1}=-6.6911eV/-6.5657eV and E_{LUMO+1}=-2.3050eV/-2.8144 eV were estimated for additional orbits. Molekülün HOMO ve Its interactions with other molecules are determined by its LUMO orbitals. Both approaches have an energy the gaps within the bands of 3.4917

eV and 3.3856 eV, with low overall values showing restricted strong chemical responsiveness and kinetic durability. The compound's band gaps are high in each approaches, showing that it is an insulator.

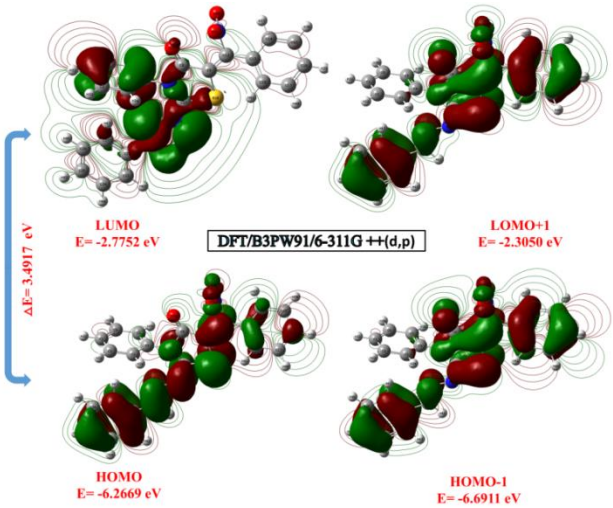

Figure 2. Thiazolidinone-Bis Schiff Base compound boundary molecular orbitals measured utilising the DFT/B3PW91/6-311++G(d,p) level

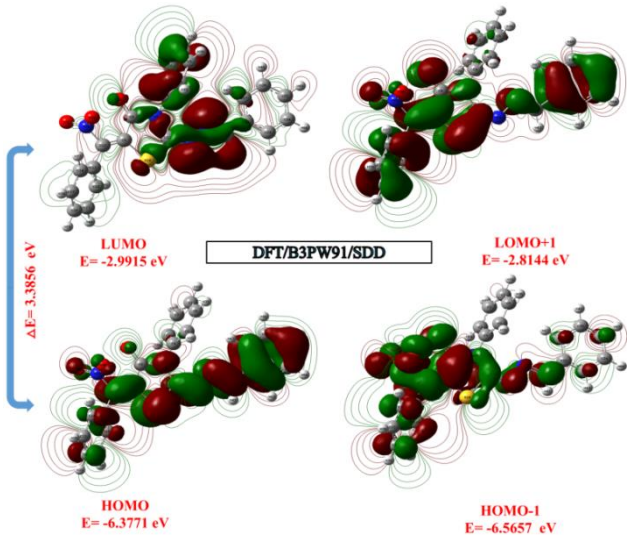

Figure 3. Thiazolidinone-Bis Schiff Base compound boundary molecular orbitals calculated using the DFT/B3PW91/SDD level

Table 3. Determining quantum chemical variables (in eV) for low energy connections by DFT/B3PW91/6-311++G(d,p)-DFT/B3PW91/SDD methods of the Thiazolidinone-Bis Schiff Base compound

Molecules Energy		**DFT/B3PW91/ 6-311++G(d,p)**	**DFT/B3PW91/ SDD**
E_{LUMO}		-2.7752	-2.9915
E_{HOMO}		-6.2669	-6.3771
E_{LUMO+1}		-2.3050	-2.8144
E_{HOMO-1}		-6.6911	-6.5657
Energy Gap	$(\Delta E)\lvert E_{HOMO}- E_{LUMO}\rvert$	3.4917	3.3856
Ionization Potential	$(I = -E_{HOMO})$	6.2669	6.3771
Electron Affinity	$(A = -E_{LUMO})$	2.7752	2.9915
Chemical hardness	$(\eta = (I - A)/2)$	1.7458	1.6928
Chemical softness	$(s = 1/2\ \eta)$	0.8729	0.8464
Chemical Potential	$(\mu = -(I + A)/2)$	-4.5210	-4.6843
Electronegativity	$(\chi = (1+ A)/2)$	1. 8876	1.9957
Electrophilicity index	$(\omega = \mu^2/2\ \eta)$	5.8538	6.4811

Molecular Electrostatic Potential (MEP)

The molecular electrostatic potential (MEP) for Thiazolidinone-Bis Schiff Base compound. displays the compound's structure, magnitude, and electrical energy levels (Sertbakan, 2021). The examination of the physical features of the atomicatomic structure becomes greatly helped by molecular electrostatic potential (MEP) mapping (Kuş, 2021). The the molecule's region having adverse electrostatic energy is vulnerable to electrophilic attack (Ergan, 2021). Various electrostatic potential values on the interface are represented in shifting hues; red and yellow show the greatest negative area that is the favored location for electrophilic agents (Ak & Kebiroglu, 2023). As demonstrated in the blue and green sections, the maximal positive range, which is the desired range of nucleophilic reactivity, is depicted by zero potential (Alkorta & Villar, 1994). The MEP map of our molecule is depicted in Figure 4. The aromatic ring region looks to be neutral (green). MEP is frequently used as a reaction map to investigate electrophilic and nucleophilic reaction regions, along with hydrogen bond interactions in organic compounds. Figure 4 shows 3D plots of our compound's MEP utilizing DFT/B3PW91/6-311++G(d,p)-DFT/B3PW91/SDD technic and foundation sets to estimate the reactive electrophilic and nucleophilic attack sites. Negative (red or yellow) parts of MEP indicate reactivity to electrophiles, whereas positive (blue) regions suggest reactivity to nucleophiles reactivity, like seen in Figure 4. These domains describe the area of the chemical where intermolecular interactions may occur. Based on these outcomes, we may conclude which H atoms have the greatest appealing, whereas O and N atoms have the most repulsive.

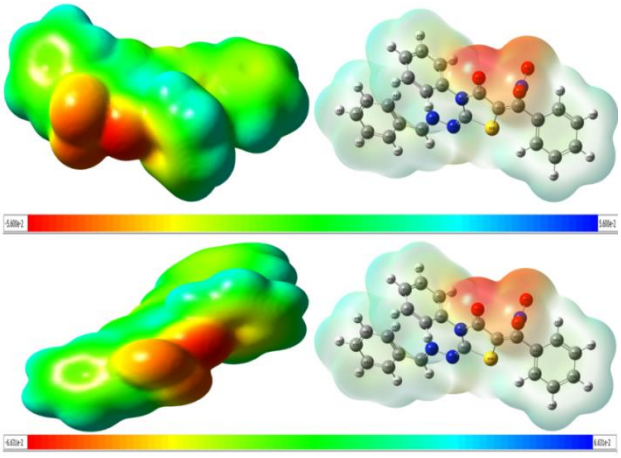

Figure 4. Molecular electrostatic potential surface of Thiazolidinone-Bis Schiff Base compound using DFT/B3PW91/6-311++G(d,p)-DFT/B3PW91/SDD methods and basis sets

Non-Linear Optical Properties (NLO)

The nonlinear optical (NLO) effect is regarded as the most important in the current study since it gives the fundamental roles of optical modification, optical changing, optical reason, and optical memory for upcoming communications networks, optical links and signals processing. The impact of the compound analyzed using DFT/B3PW91/6-311++G(d,p)-DFT/B3PW91/SDD techniques on NLO characteristics were evaluated by calculating dipole moments (μ), polarizability, anisotropy of polarizability (α), and average first-order hyperpolarization (β) was calculated utilizing the finite field approach and is shown in Table 4. Because the GAUSSIAN09W output's average polarizability and average first-order hyperpolarizability have been presented in atomic units (a.u.), the estimated amounts were allocated to electrostatic units (esu) (α:1 a.u=0,1482×10^{-24} esu; β:1 a.u.=8,6393×10^{-33} esu) (Mahmood et al., 2015). As is given in Table 4, the computed dipole moment for the DFT/B3PW91/6-311++G(d,p) stage was 5.3876, essentially regardless of the base set, and the greater dipole moment in

the examined compound was mostly due to this. The y component has the largest magnitude of the dipole moment. As shown in Table 4, diagonal components dominate the computed polarization values. The the computed polarizability and anisotropy of polarizability parameters are equal to $3.49x10^{-30}$ ve $3.53x10^{-30}$ esu for the DFT/B3PW91/6-311++G(d,p)-DFT/B3PW91/SDD technic. The following equations (1-3) were utilized to computed the average polarizability (α), dipole moment (μ), and molecule hyperpolarizability parameters.

$$\mu = (\mu_x^2 + \mu_z^2)^{1/2} \quad (1)$$

$$\beta_{Total} = (\beta^2 x + \beta^2 y + \beta^2 z)^{1/2} \quad (2)$$

$$= [(\beta xxx + \beta xyy + \beta xzz)^2 + (\beta yyy + \beta yxx + yzz)^2 + (\beta zzz + \beta zxx + \beta zyy)^2]^{\frac{1}{2}} \quad (3)$$

Table 4. The polarizability (au), dipole moments (Debye), components, and total value of Thiazolidinone-Bis Schiff Base compound are calculated utilising DFT/B3PW91/6-311++G(d,p)-DFT/B3PW91/SDD technique and basis sets

Parameters	B3PW91/ 6-311G++(d,p)	B3PW91/ SDD	Parameters	B3PW91/ 6-311G++(d,p)	B3PW91/ SDD
μ_x	-2.5215	-3.5118	β_{XXX}	5.3987	-26.5815
μ_y	-4.7605	-4.7615	β_{YYY}	-57.1613	-59.5056
μ_z	-0.0780	-0.0150	β_{ZZZ}	3.6908	4.8385
$\mu_{(D)}$	5.3876	5.9165	β_{XYY}	-76.6193	-82.0364
α_{XX}	-149.8715	-142.0664	β_{XXY}	-134.5963	-137.2040
α_{YY}	-187.7894	-183.5958	β_{XXZ}	-49.1712	-46.1480
α_{ZZ}	-187.6668	-184.1032	β_{XZZ}	16.0136	8.1528
α_{XY}	-30.1883	-28.8540	β_{YZZ}	24.5644	23.2150
α_{XZ}	-4.2343	-3.4767	β_{YYZ}	8.6048	7.6956
α_{YZ}	-4.1991	-3.7350	β_{XYZ}	-18.9666	-19.5031
α (au)	-181.375	-182.456	β (esu)	$3.49x10^{-30}$	$3.53x10^{-30}$

NBO Analysis

NBO analysis was done on the optimized structures to further comprehend the intermolecular interactions in the LASP molecule. The Gaussian 09W program package's NBO analysis software was utilized. The DFT/B3PW91/6-311++G(d,p) assumption is employed in the comparisons in Table 4 to indicate the percentages of individual bond electrons in various bonds, as well as variations in the percentages of electrons in the s, p, and d orbitals in each atom (Kurt et al., 2011). For Thiazolidinone-Bis Schiff Base, a quadratic equation is applied. The relationship between the recipient (j) and the transmitter (i) has been estimated utilising Fock marix (Govindarajan & Karabacak, 2012). For every donor (i) and receiver (j), the stabilizing value related to delocalization is projected to be as follows (Sosa et al., 2002).

$$E(2) = \Delta Eij = qi \frac{(Fi,j)^2}{(\mathcal{E}i - \mathcal{E}j)} \quad (4)$$

Natural bond orbital (NBO) studies is a powerful method for investigating intramolecular and intermolecular bonds, addition to the interaction between bonds. It also serves like a solid platform to investigating charge transfer or conjugative interaction in molecular structures (Eşme & Sağdınç, 2017). The second-order Fock matrix has been used to examine various sorts of donor-acceptor connections and their NBO-based balancing powers. The interaction results in a absence of occupation from the hypothetical Lewis structure's localized NBO to an empty non-Lewis orbital. The balancing powers E(2) Concerned with electron delocalization between donor and acceptor for every one donor NBO (i) and acceptor NBO (j) is given by where i q is the donor-orbital occupancy, j and i are diagonal orbital elements is approximated as follows (Kolandaivel & Nirmala, 2004). The bigger the value of E(2), the

the stronger the connection between electron donors and acceptors, i.e., the higher the proclivity of electron electrons to be donated by donors and the higher the degree of the pairing of Acceptors and the overall network (Pathak et al., 2015). Table 5 shows the results of NBO analysis to reveal the intramolecular interaction, rehybridization, and delocalization of electron density inside the structure. The stability energies of our molecule have been estimated utilising second-order perturbation analysis to study the intramolecular interaction. There is a substantial intramolecular hyperconjugative contact of -electrons with larger energy contributions than C4 in the molecule C1–C6→C4–C5 (44.87 kcal/mol for DFT/B3PW91 level). N29-O31 (16.29 kcal/mol for DFT/B3PW91 level), C22–C23→N20–C23 (22.24 kcal/mol for DFT/B3PW91 level), C2–C3 (44.87 kcal/mol for DFT/B3PW91 level). C11–N19→N20–C21 has a DFT/B3PW91 level of 16.45 kcal/mol.

Table 5. Selected NBO results of Thiazolidinone-Bis Schiff Base are determined utilising the 6-311++G(d,p) basis set utilising the DFT/B3PW91 technique

NBO(i)	Type	Occupancies	NBO(j)	Type	Occupancies	E(2)[a] (Kcal/mol)	E (j)-E(i)[b] (a.u.)	F (i, j)[c] (a.u)
C1-C2	σ	1.98005	**C2-C3**	σ*	0.32065	4.28	1.78	0.078
C1-C6	σ	1.98007	**C5-C6**	σ*	0.01581	4.28	1.78	0.078
C1-C6	π	1.66059	**C4-C5**	π*	0.35534	44.87	0.47	0.130
C2-C3	σ	1.97657	**C3-C4**	σ*	0.02356	4.70	1.78	0.082
C2-C3	π	1.65582	**C1-C6**	π*	0.01612	43.22	0.47	0.128
C3-H34	σ	1.98248	**C3-C4**	σ*	0.02356	3.73	1.55	0.068
C3-C4	σ	1.97592	**C4-C5**	σ*	0.35534	6.78	1.80	0.098
C4-C5	σ	1.97594	**C5-C6**	σ*	0.01581	4.29	1.80	0.079
C4-C5	π	1.67326	**C2-C3**	π*	0.32065	42.89	0.49	0.130
N7-C8	σ	1.98355	**N7-C11**	σ*	0.05578	3.71	1.62	0.070
C5-C6	σ	1.97659	**C8-S10**	σ*	0.02270	5.18	1.52	0.079
N7-C8	σ	1.98355	**C11-N19**	σ*	0.01089	4.36	1.89	0.081
C8-C9	σ	1.97691	**C9-C12**	σ*	0.16866	6.76	1.82	1.82
C8-O28	π	1.98360	**C9-C12**	π*	0.16866	6.07	0.68	0.060
C9-S10	σ	1.96971	**C12-N29**	σ*	0.08210	6.90	1.31	0.086
C9-C12	π	1.91573	**C8-O28**	π*	0.20382	22.24	0.59	0.105
S10-C11	σ	1.97211	**N19-C21**	σ*	0.00537	6.37	1.48	0.087
C11-N19	π	1.99207	**N20-C21**	π*	0.11946	16.45	0.66	0.094
C12-C13	σ	1.96861	**N29-O31**	π*	0.54467	2.27	0.89	0.046
C13-C14	σ	1.97185	**C13-C18**	σ*	0.02375	6.50	1.75	0.095
C13-C18	π	1.66149	**C9-C12**	π*	0.16866	17.06	0.47	0.084
C14-C15	π	1.97872	**C16-C17**	π*	0.31551	43.97	0.48	0.131
C15-C16	σ	1.98041	**C14-C15**	σ*	0.01569	4.27	1.78	0.078
C16-C17	π	1.64248	**C13-C18**	π*	0.38398	50.02	0.46	0.136
C17-C18	σ	1.97858	**C13-C18**	σ*	0.02375	5.13	1.75	0.085
N19-N20	σ	1.97938	**C21-C22**	σ*	0.02432	4.48	1.78	0.080
N20-C21	π	1.99168	**C22-C23**	π*	0.37189	11.28	0.59	0.079
C22-C23	σ	1.97485	**N20-C23**	σ*	0.00537	26.33	0.49	0.108

Molecular Docking Studies

A computer-generated 3D structure of small ligands has been docked into a receptor molecule in conformations, multiple orientations, and locations via molecular docking. This approach is important in drug development and medicinal chemistry since it provides information on molecular recognition (Shoichet et al., 2002). Docking is now an essential component of Computer Aided Drug Design and Discovery (CADDD). Conventional docking approaches have difficulties in semiflexible or static target and ligand processing (Abdelsattar et al., 2021). In the past decade, developments in computation, genomics, and proteomics have also resulted in the creation of several docking approaches that integrate protein-ligand adaptability and their many binding configurations. The flexibility of receptors allows for more precise binding posture predictions and a more reasonable representation of ligand and protein binding interactions (Baskaran & Ramachandran, 2012). Protein flexibility has been achieved through the use of protein ensembles or dynamic docking approaches. Schiff Thiazolidinone Molecular docking

results toward urease enzymes and cancer were obtained. The complexes of proteins of these enzymes have been discovered by investigating the online resource RSCB protein database for 4UXL and 4UBF. To establish the tying pattern of contacts with enzyme websites, molecular docking experiments were done using several technologies (AutoDock, Discovery Studio Visualizer). The docking score of the Thiazolidinone-Bis Schiff Base complex has shown in Table 6. The visualized findings for the molecule in issue, as well as the interaction and distances of the ligands, are shown in Figures 5 and 6. GLU-1997, LEU-2026, and MET-2001 are van der Waals bonded hydrogen in our compound's binding process. LYS-1980 (4.59 Å) is hydrogen bound using standard hydrogen bonds. VAL-1959 (5.75 Å) binds the Pi-Alkyl thiazolidine ring, while LEU-2086 (5.39 Å) and ALA-1978 (5.82 Å) bind the Pi-Alkyl nitrovinyl benzene ring. Unfavorable negative-negative ASP-2033 (5.39 Å). Carbon hydrogen bonds join ASP-2102 (3.51 Å) and GLY-2032 (3.41 Å).

Table 6. Docking score of Thiazolidinone-Bis Schiff Base compound PDB: 4UXL and PDB: 4UBF

Compound	Docking Score	
	(PDB: 4UXL)	(PDB: 4UBF)
Thiazolidinone-Bis Schiff Base	-6.865	-7.980

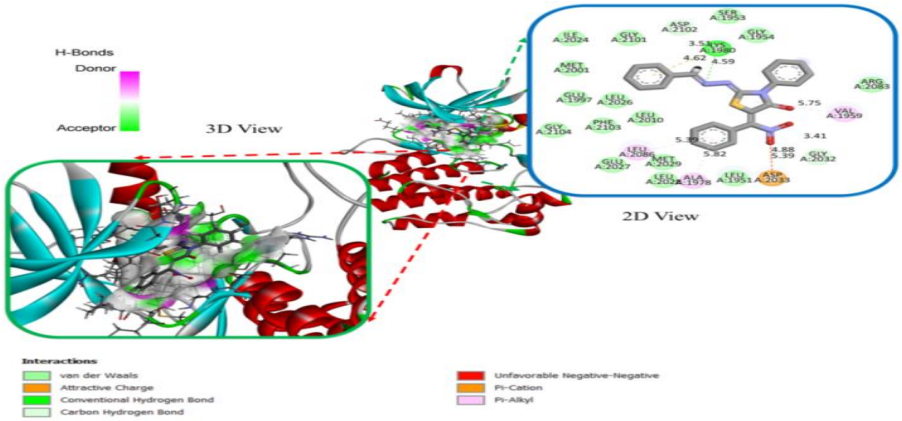

Figure 5. 3D illustration of the aromatic region of the receptor and a 2D picture of the 4UXL enzyme interactions

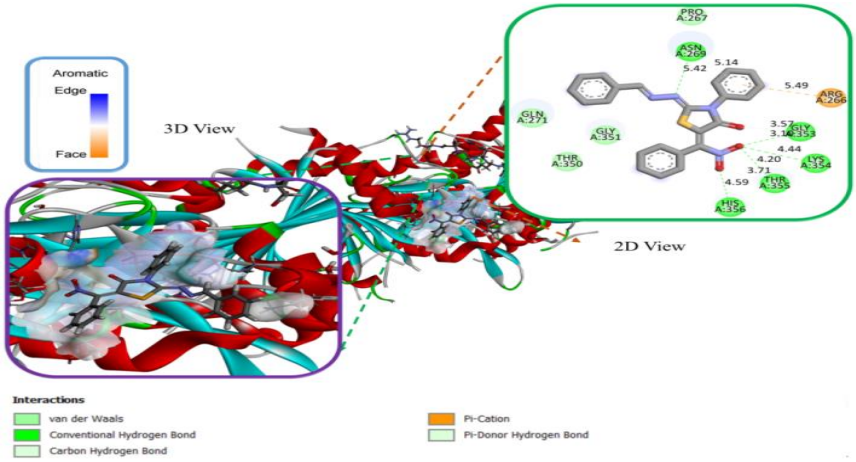

Figure 6. 3D illustration of the aromatic region of the receptor and a 2D picture of the 4UBF enzyme interactions

CONCLUSION

The Thiazolidinone-Bis Schiff Base compound was studied in depth using quantum chemical computations. The compound's structural structure was predicted using B3PW91/6-311G++(d,p) and B3PW91/SDD levels of approach. The structure's dihedral angles, bond lengths, and bond angles were

in theory specified building properties. The molecule's nonlinear optical characteristics have been also investigated. It was also established that the chemical under consideration might be employed for an NLO material. There are also HOMO-LUMO, Mulliken atomic charges, and MEP maps displayed. The Thiazolidinone-Bis Schiff Base molecule was also docked to examine the particular binding position and the ligand activity on the protein. Binding approaches were investigated after determining the appropriate exposure for total ligand-enzyme docking to better understand the inhibitory processes. The shift scores in binding affinity with 4UXL and 4UBF were determined in the research to be -6.865 kcal/mol and -7.980 kcal/mol. It is more effective with the 4UBF binding receptor score. Because this molecular structure has strong therapeutic potential, we believe it may be utilized to produce innovative drugs for cancer and urease therapy, in addition to a novel enzyme inhibitor option.

Conflict of Interest

The article authors declare that there is no conflict of interest between them.

Author's Contributions

The authors declare that they have contributed equally to the article

REFERENCES

Abdelsattar, A. S., Dawoud, A., & Helal, M. A. (2021). Interaction of nanoparticles with biological macromolecules: a review of molecular docking studies. *Nanotoxicology*, *15*(1), 66-95.

Ak, F., & Kebiroglu, H. (2023). Molecular Structure, Geometry Properties, HOMO-LUMO, and MEP Analysis of Acrylic Acid Based on DFT Calculations. *Journal of Physical Chemistry and Functional Materials*, *6*(2), 92-100.

Al-Sharif, M. S. (2023). 2,4-dihydroxybenzaldehyde based Schiff base derivatives as an effective corrosion inhibitor for steel corrosion in 1 M hydrochloric acid solution. *International Journal of Electrochemical Science*, *18*(12), 100384.

Alkorta, I., & Villar, H. O. (1994). Molecular electrostatic potential of D1 and D2 dopamine agonists. *Journal of Medicinal Chemistry*, *37*(1), 210-213.

Assfeld, X., & Rivail, J.-L. (1996). Quantum chemical computations on parts of large molecules: the ab initio local self consistent field method. *Chemical Physics Letters*, *263*(1), 100-106.

Baskaran, C., & Ramachandran, M. (2012). Computational molecular docking studies on anticancer drugs. *Asian Pacific Journal of Tropical Disease*, *2*, S734-S738.

Berhanu, A. L., Gaurav, Mohiuddin, I., Malik, A. K., Aulakh, J. S., Kumar, V., & Kim, K.-H. (2019). A review of the applications of Schiff bases as optical chemical sensors. *TrAC Trends in Analytical Chemistry*, *116*, 74-91.

Callahan, B. P., Yuan, Y., & Wolfenden, R. (2005). The Burden Borne by Urease. *Journal of the American Chemical Society*, *127*(31), 10828-10829.

Cuesta, I. G., Pedersen, T. B., Koch, H., & Sánchez de Merás, A. (2006). Carbon Nanorings: A Challenge to Theoretical Chemistry. *ChemPhysChem*, *7*(12), 2503-2507.

da Silva, C. M., da Silva, D. L., Modolo, L. V., Alves, R. B., de Resende, M. A., Martins, C. V. B., & de Fátima, Â. (2011). Schiff bases: A short review of their antimicrobial activities. *Journal of Advanced Research*, *2*(1), 1-8.

Demir, P., & Akman, F. (2017). Molecular structure, spectroscopic characterization, HOMO and LUMO analysis of PU and PCL grafted onto PEMA-co-PHEMA with DFT quantum chemical calculations. *Journal of Molecular Structure*, *1134*, 404-415.

El-Hassab, M. A. E.-M., El-Bastawissy, E. E., & El-Moselhy, T. F. (2020). Identification of potential inhibitors for HCV NS5b of genotype 4a by combining dynamic simulation, protein–ligand interaction fingerprint, 3D pharmacophore, docking and 3D QSAR. *Journal of Biomolecular Structure and Dynamics*, *38*(15), 4521-4535.

Ergan, E. (2021). Theoretical Studies via DFT Calculation of Pyrimidine Derivatives as Potential Corrosion Inhibitor [Potansiyel Korozyon İnhibitörü Olarak Pirimidin Türevlerinin DFT Hesaplaması ile Teorik Çalışmalar]. *Journal of the Institute of Science and Technology*, *11*(3), 2142-2151.

Eşme, A., & Sağdınç, S. G. (2017). Spectroscopic (FT–IR, FT–Raman, UV–Vis) analysis, conformational, HOMO-LUMO, NBO and NLO calculations on monomeric and dimeric structures of 4-pyridazinecarboxylic acid by HF and DFT methods. *Journal of Molecular Structure*, *1147*, 322-334.

Goh, G. B., Hodas, N. O., & Vishnu, A. (2017). Deep learning for computational chemistry. *Journal of Computational Chemistry*, *38*(16), 1291-1307.

Govindarajan, M., & Karabacak, M. (2012). Spectroscopic properties, NLO, HOMO–LUMO and NBO analysis of 2,5-Lutidine. *Spectrochimica Acta Part A: Molecular and Biomolecular Spectroscopy*, *96*, 421-435.

Hodnett, E. M., & Dunn, W. J. (1970). Structure-antitumor activity correlation of some Schiff bases. *Journal of Medicinal Chemistry*, *13*(4), 768-770.

Hratchian, H. P., Parandekar, P. V., Raghavachari, K., Frisch, M. J., & Vreven, T. (2008). QM:QM electronic embedding using Mulliken atomic charges: Energies and analytic gradients in an ONIOM framework. *The Journal of Chemical Physics*, *128*(3).

Kaltsoyannis, N. (2018). Transuranic Computational Chemistry. *Chemistry – A European Journal*, *24*(12), 2815-2825.

Kar, T., & Sannigrahi, A. B. (1988). Effect of basis set on Mulliken and Löwdin atomic charges, bond orders and valencies of some polar molecules. *Journal of Molecular Structure: THEOCHEM*, *165*(1), 47-54.

Kolandaivel, P., & Nirmala, V. (2004). Study of proper and improper hydrogen bonding using Bader's atoms in molecules (AIM) theory and NBO analysis. *Journal of Molecular Structure*, *694*(1), 33-38.

Kurt, M., Babu, P. C., Sundaraganesan, N., Cinar, M., & Karabacak, M. (2011). Molecular structure, vibrational, UV and NBO analysis of 4-chloro-7-nitrobenzofurazan by DFT calculations. *Spectrochimica Acta Part A: Molecular and Biomolecular Spectroscopy*, *79*(5), 1162-1170.

Kuş, N. (2021). Orbıtal Interactıons and Stabılızatıon Energıes of Methyl 5-6 Dihydro Benzo(H) Quınolıne-4-Carboxylate [Orbital interactions and stabilization energies of methyl 5-6 dihydro benzo(h) quinoline-4-carboxylate]. *Eskişehir Teknik Üniversitesi Bilim ve Teknoloji Dergisi B - Teorik Bilimler*, *9*(Iconat Special Issue 2021), 74-84.

Mahmood, A., Khan, S. U.-D., Rana, U. A., Janjua, M. R. S. A., Tahir, M. H., Nazar, M. F., & Song, Y. (2015). Effect of thiophene rings on UV/visible spectra and non-linear optical (NLO) properties of triphenylamine based dyes: a quantum chemical perspective. *Journal of Physical Organic Chemistry*, *28*(6), 418-422.

Michael J. Frisch, T., G.W, Bernhard Schlegel, Gustavo Scuseria. (2016). *Gaussian 09*. In *Revision E.01*

Mobley, H. L. T. (2001). Urease. In *Helicobacter pylori* (pp. 177-191).

Pang, Z.-H., & Reed, M. (1998). Theoretical Chemical Thermometry on Geothermal Waters: Problems and Methods. *Geochimica et Cosmochimica Acta*, *62*(6), 1083-1091.

Parandekar, P. V., Hratchian, H. P., & Raghavachari, K. (2008). Applications and assessment of QM:QM electronic embedding using generalized asymmetric Mulliken atomic charges. *The Journal of Chemical Physics*, *129*(14).

Pathak, S. K., Srivastava, R., Sachan, A. K., Prasad, O., Sinha, L., Asiri, A. M., & Karabacak, M. (2015). Experimental (FT-IR, FT-Raman, UV and NMR) and quantum chemical studies on molecular structure, spectroscopic analysis, NLO, NBO and reactivity descriptors of 3,5-Difluoroaniline. *Spectrochimica Acta Part A: Molecular and Biomolecular Spectroscopy*, *135*, 283-295.

Polacco, J. C., & Holland, M. A. (1993). Roles of Urease in Plant Cells. In K. W. Jeon & J. Jarvik (Eds.), *International Review of Cytology* (Vol. 145, pp. 65-103). Academic Press.

Preeti, Jaiswal, A., Kumar, M., & Singh, K. N. (2023). An Efficient Combinatorial Synthesis of Novel Thiazolidinone-Bis Schiff Base Hybrids Using One-Pot Multicomponent Reaction. *Asian Journal of Organic Chemistry*, *12*(2), e202200629.

Pyykkö, P. (2005). Theoretical chemistry of gold. II. *Inorganica Chimica Acta*, *358*(14), 4113-4130.

Qin, Y., & Cabral, J. M. S. (2002). Review Properties and Applications of Urease. *Biocatalysis and Biotransformation*, *20*(1), 1-14.

Rupp, M., Von Lilienfeld, O. A., & Burke, K. (2018). Guest Editorial: Special Topic on Data-Enabled Theoretical Chemistry. *The Journal of Chemical Physics*, *148*(24).

Sertbakan, T. R. (2021). 4-Amino-2-Metil-7(Triflorometil)Kinolin Molekülünün Bazı Özelliklerinin Deneysel ve Teorik Spektroskopik Yöntemlerle İncelenmesi [Investigation of some properties of 4-amino-2-methyl-7(trifluoromethyl)quinoline molecule by experimental and theoretical spectroscopic methods]. *Journal of Anatolian Physics and Astronomy*, *1*(2), 46-64.

Shoichet, B. K., McGovern, S. L., Wei, B., & Irwin, J. J. (2002). Lead discovery using molecular docking. *Current Opinion in Chemical Biology*, *6*(4), 439-446.

Sosa, G. L., Peruchena, N. M., Contreras, R. H., & Castro, E. A. (2002). Topological and NBO analysis of hydrogen bonding interactions involving C–H···O bonds. *Journal of Molecular Structure: THEOCHEM*, *577*(2), 219-228.

Suhasini, M., Sailatha, E., Gunasekaran, S., & Ramkumaar, G. R. (2015). Vibrational and electronic investigations, thermodynamic parameters, HOMO and LUMO analysis on Lornoxicam by density functional theory. *Journal of Molecular Structure*, *1100*, 116-128.

Tabatabai, M. A., & Bremner, J. M. (1972). Assay of urease activity in soils. *Soil Biology and Biochemistry*, *4*(4), 479-487.

Topsom, R. D. (1983). Contribution of theoretical chemistry to an understanding of electronic substituent effects. *Accounts of Chemical Research*, *16*(8), 292-298.

Verma, A., Kumar, V., Naik, B., Masood Khan, J., Singh, P., Erik Joakim Saris, P., & Gupta, S. (2023). Screening and molecular dynamics simulation of compounds inhibiting MurB enzyme of drug-resistant Mycobacterium tuberculosis: An in-silico approach. *Saudi Journal of Biological Sciences*, *30*(8), 103730.